Cell and Tissue Research
https://doi.org/10.1007/s00441-024-03907-5

RESEARCH

Involvement of vimentin- and BLBP-positive glial cells and their MMP expression in axonal regeneration after spinal cord transection in goldfish

Akihito Takeda[1] · **Minami Teshima**[1] · **Kengo Funakoshi**[1]

Received: 19 May 2024 / Accepted: 19 July 2024

Abstract
In goldfish, spinal cord injury triggers the formation of a fibrous scar at the injury site. Regenerating axons are able to penetrate the scar tissue, resulting in the recovery of motor function. Previous findings suggested that regenerating axons enter the scar through tubular structures surrounded by glial elements with laminin-positive basement membranes and that glial processes expressing glial fibrillary acidic protein (GFAP) are associated with axonal regeneration. How glia contribute to promoting axonal regeneration, however, is unknown. Here, we revealed that glial processes expressing vimentin or brain lipid-binding protein (BLBP) also enter the fibrous scar after spinal cord injury in goldfish. Vimentin-positive glial processes were more numerous than GFAP- or BLBP-positive glial processes in the scar tissue. Regenerating axons in the scar tissue were more closely associated with vimentin-positive glial processes than GFAP-positive glial processes. Vimentin-positive glial processes co-expressed matrix metalloproteinase (MMP)-14. Our findings suggest that vimentin-positive glial processes closely associate with regenerating axons through tubular structures entering the scar after spinal cord injury in goldfish. In intact spinal cord, ependymo-radial glial cell bodies express BLBP and their radial processes express vimentin, suggesting that vimentin-positive glial processes derive from migrating ependymo-radial glial cells. MMP-14 expressed in vimentin-positive glial cells and their processes might provide a beneficial environment for axonal regeneration.

Keywords Teleost · Radial glia · Vimentin · Brain lipid-binding protein · Matrix metalloproteinase

Introduction

Spinal cord injury (SCI) in adult mammals produces a negative environment for the severed nerves at the injury site, including inflammation, scar formation, and a large cavity, which inhibits axonal outgrowth. Functional recovery after SCI is thus poor in mammals, and no fundamental treatment for SCI is available in humans. In several teleost species, however, such as goldfish (Koppanyi 1955; Sharma et al. 1993; Takeda et al. 2007), zebrafish (Becker et al. 1997, 2004), and knifefish (*Apteronotus leptorhynchus*: Vitalo et al. 2016), spontaneous axonal regeneration occurs across the injury site after SCI, resulting in the recovery of motor function.

The mechanisms of spontaneous axonal regeneration and functional recovery in teleosts remain unclear. In goldfish, a fibrous scar filled with collagen forms at the injury site after spinal cord transection (SCT), and regenerating axons penetrate the fibrous scar through tubular structures that form within the fibrous scar tissue (Bernstein 1964; Bernstein and Bernstein 1967; Takeda et al. 2015). The tubular structures protrude into the fibrous scar from the surrounding nerve tissue, and their walls are composed of laminin continuous with the basement membrane bordering the fibrous scar and surrounding nervous tissue. As the tubules enlarge, the number of regenerating axons increases and the fibrous scar area becomes smaller (Takeda et al. 2015). Details regarding the organization of the fibrous scar tissue and the tubular structures that develop therein are provided in Takeda et al. (2015).

The cellular and non-cellular factors that promote the outgrowth of regenerating axons, however, are not well understood. After SCI in teleost, a variety of cells, including glial cells, are activated and various substances are released (Becker and Becker 2020; Zupanc 2019). A previous study

✉ Kengo Funakoshi
funako@yokohama-cu.ac.jp

[1] Department of Neuroanatomy, Yokohama City University School of Medicine, 3-9 Fukuura, Kanazawa-Ku, Yokohama 236-0004, Japan

Published online: 09 August 2024

demonstrated that regenerating axons are frequently accompanied by glial processes within the tubular structures in goldfish (Takeda et al. 2015). Elongation of glial fibrillary acidic protein (GFAP)–positive glial processes is frequently preceded by the regenerating axons, suggesting that GFAP-positive glial processes do not guide the axonal regrowth (Nona and Stafford 1995). These observations raise the possibility that axonal regeneration is not guided by glial factors. Alternatively, GFAP-negative glial elements might be involved in axonal outgrowth (Takeda et al. 2015).

Ependymo-radial glial cells in the ependymal layer are suggested to contribute to axonal regeneration after SCT in some anamniotes. In zebrafish, a species closely related to goldfish, scar tissue is not formed after SCT. Instead, the gap in the spinal cord is reconnected by glial bridges created by the migration of ependymo-radial glial cells that normally express GFAP but proliferate and de-differentiate to transiently express vimentin following SCT (Goldshmit et al. 2012). The ependymo-radial glial cells and their processes in the bridges, therefore, provide a scaffold for regenerating axons to pass through the injury site, but whether these cells promote axonal regeneration on the glial bridges remains unclear (Tsata et al. 2021). In some teleosts, on the other hand, the ependymo-radial glial cells strongly express vimentin together with GFAP. Although GFAP and vimentin colocalize in many areas, there are many areas in which they do not coexist (Arochena et al. 2004; Zupanc et al. 2012). Brain lipid-binding protein (BLBP) is also suggested to be expressed in ependymo-radial glial cells in teleosts (Adolf et al., 2006; Wen et al. 2010).

In the present study, we further investigated the possible involvement of glial elements in the outgrowth of regenerating axons in goldfish by evaluating the morphological relationship between regenerating axons and glial elements in the fibrous scar, using glial markers other than GFAP, such as vimentin and BLBP. Vimentin and BLBP might be expressed in cell types distinct from glial cells expressing GFAP. We also re-examined the expression of matrix metalloproteinases (MMPs) in glial processes entering the fibrous scar, based on previous observations that GFAP-positive glial processes express MMP-14 after SCT (Takeda et al. 2021).

Materials and methods

Spinal cord hemisection

Goldfish, *C. auratus* ($n = 12$; body weight 20–30 g), were obtained commercially (Nomoto Fish Farm Co. Ltd., Yokohama, Japan) and maintained in an aquarium at 25–27 °C. A total of 6 fish underwent SCT in this study. For better quantitative evaluation of the regenerating axons and behavioral activities, a lateral hemisection was performed because full transection at the upper spinal level frequently leads to permanent separation of the spinal cord. Lateral hemisection is a useful model for sequential observation of regenerating axons (Takeda et al. 2007, 2015). The fish were deeply anesthetized with 0.02% tricaine methanesulfonate (MS-222, Millipore Sigma, St. Louis, MO, USA) in water and placed on ice. The dorsal skin was incised at the level just caudal to the cranium, the muscles retracted, and the post-temporal bone and vertebrae exposed. The rostral segments of the spinal cord were exposed after removing the bones, and a frontal hemisection on the left side of the spinal cord was performed at the level of the first spinal nerve. The hemisection was achieved by inserting the blades of small scissors at a right angle to the spinal surface along the posterior median septum. After the wound was sutured and sealed with an aerosol plastic dressing (Yoshitomi-Seiyaku, Osaka, Japan), the fish was placed in a bucket of water until the anesthesia wore off and then placed in 0.1% tetracycline for approximately 15 min and returned to the aquarium.

Perfusion, fixation, and tissue preparation

Fish at 3 days ($n = 3$) and 7 days ($n = 3$) after SCT were processed for immunohistochemistry. The fish were anesthetized and perfused transcardially with saline containing 1% heparin, followed by 0.1 M phosphate buffer (PB, pH 7.4) containing 4% paraformaldehyde (PFA). The spinal cord, including the injury site, was removed immediately, post-fixed in 0.1 M PB containing 4% PFA for 5 to 6 h at 4 °C, and left overnight in 0.1 M PB containing 25% sucrose at 4 °C for cryoprotection.

The spinal cord was embedded in Tissue-Tek OCT compound (Sakura, Tokyo, Japan) and frozen with 2-methylbutane (isopentane) in liquid nitrogen. The frozen specimens were cut into serial 20-μm thick horizontal sections and thaw-mounted on gelatin-coated slides in a cryostat (Moriyasu-Konetsu, Osaka, Japan) equipped with a microtome (Microm, Walldorf, Germany). The sections were arranged in a 1 in 5 series comprising every fifth section. A series comprised 10 to 12 sections. All sections were dried for 1 h at room temperature, postfixed in 0.1 M PB containing 4% PFA for 30 min, and rinsed in 0.01 M PBS (pH 7.4) containing 0.3% Triton X-100 (PBST, pH 7.4) for 10 to 20 min.

Immunostaining

A series of sections were incubated in a moist chamber overnight for 3 nights at 4 °C with a mixture of primary antibodies diluted with 1% normal donkey serum, 0.2% bovine serum albumin, and 0.1% NaN3 in 0.01 M PBST. The primary antibodies were as follows: (1) mouse monoclonal anti-acetylated tubulin (1:100, T7451, Sigma-Aldrich,

Darmstadt, Germany, RRID: AB_609894) as an axonal marker for axons; (2) goat polyclonal anti-GFAP (1:100, ab53554, Abcam, Cambridge, UK, RRID: AB_880202); (3) mouse monoclonal anti-vimentin (1:200, ab8069, Abcam, RRID: AB_306239); (4) rabbit polyclonal anti-vimentin (1:50, ab229622, Abcam, RRID: none); (5) rabbit polyclonal anti-BLBP (1:300, ABN14, Millipore, Burlington, MA, USA, RRID: AB_10000325); (6) rabbit polyclonal anti-MMP-9 (1:50, AS55345, AnaSpec, Fremont, CA, USA, RRID: AB_2144746); and (7) rabbit polyclonal anti-MMP-14 (1:50, ab53712, Abcam, RRID: AB_881233). The antibody combinations for multiple labeling were as follows: (1) anti-acetylated tubulin, anti-GFAP, and anti-vimentin; (2) anti-BLBP, anti-GFAP, and anti-vimentin; (3) anti-GFAP, anti-MMP-9, and anti-vimentin; and (4) anti-GFAP, anti-MMP-14, and anti-vimentin.

The sections were rinsed several times with 0.01 M PBST, and then incubated for 3 h at room temperature with a mixture of secondary antibodies diluted with 1% normal donkey serum, 0.2% bovine serum albumin, and 0.1% NaN3 in 0.01 M PBST. The secondary antibodies were as follows: (1) Alexa 488–conjugated donkey anti-rabbit IgG (10 µg/ml; Jackson ImmunoResearch Laboratories, West Grove, PA, USA); (2) cyanine Cy3–conjugated donkey anti-rabbit IgG (10 µg/ml; Jackson ImmunoResearch Laboratories); (3) Alexa 647–conjugated donkey anti-rabbit IgG (10 µg/ml; Jackson ImmunoResearch Laboratories); (4) cyanine Cy3–conjugated donkey anti-mouse IgG (10 µg/ml; Jackson ImmunoResearch Laboratories); (5) Alexa 647–conjugated donkey anti-rabbit IgG (10 µg/ml; Jackson ImmunoResearch Laboratories); (6) cyanine Cy3–conjugated donkey anti-goat IgG (10 µg/ml; Jackson ImmunoResearch Laboratories); and (7) Alexa 647–conjugated donkey anti-goat IgG (10 µg/ml; Jackson ImmunoResearch Laboratories).

Verification of antibody specificity

The negative control study for immunohistochemistry was performed by incubating spinal cord sections with 0.5% normal mouse serum (Jackson ImmunoResearch Laboratories), 0.5% normal rabbit serum (Jackson ImmunoResearch Laboratories), or 0.5% normal goat serum (Jackson ImmunoResearch Laboratories) instead of the primary antibodies. Frozen sections were fixed in 4% PFA for 5 min.

Antibodies against MMP-9 (AS55345, AnaSpec, RRID: AB_2144746) and vimentin (ab229622, Abcam) were generated using the tissue of zebrafish, a closely related species of goldfish. The antibody against GFAP (ab53554, Abcam, RRID: AB_880202) was confirmed to react specifically with antigens in zebrafish tissue and was used for goldfish studies (Takeda et al. 2021, 2023). The antibody against acetylated tubulin (T7451, Sigma-Aldrich, RRID: AB_609894) was confirmed to react specifically with antigens in the tissue of various mammalian species, frog, chicken, and invertebrates, and used in studies of zebrafish (Wilson et al. 1990), and goldfish (Takeda et al. 2021, 2023). To confirm the specificity of antibodies against MMP-14 (ab53712, Abcam, RRID: AB_881233), vimentin (ab8069, Abcam, RRID: AB_306239), and BLBP (ABN14, Millipore, RRID: AB_10000325), the amino acid sequence of the antigenic site of each antibody and the amino acid sequence homologous to the antigenic site of zebrafish were obtained from the NCBI protein database (Bethesda, MD, USA). The obtained homologous sequences were locally aligned by EMBOSS Water (EMBL-EBI, Hinxton, UK), and the amino acid match rates were calculated to be 78% for MMP-14, 88% for vimentin (mouse), and 92% for BLBP.

Observation and imaging

All sections were examined using an epifluorescence microscope (Leica DMR; Leica, Wetzlar, Germany) equipped with appropriate fluorescence filter sets. Images obtained with a CCD camera (Leica DC 20; Leica) were digitally transferred to a computer using DC Viewer Software (Leica). The spinal region of the first spinal segment, 0–2 mm caudal to the medullospinal junction was observed as the intact site. The spinal region on the transected (left) side, from the level 0.5 mm rostral to the transected site to the level 0.5 mm caudal to the transected site, was observed as the injury site.

Quantitative analysis of the number of glial processes within the fibrous scar

To quantitatively analyze the number of glial processes entering the fibrous scar, we used a series of spinal cord sections stained with anti-acetylated tubulin, anti-GFAP, and anti-vimentin, obtained from the fish 3 days ($n=3$) and 7 days ($n=3$) after SCT. The numbers of acetylated tubulin-immunoreactive axonal processes, GFAP-immunoreactive glial processes, and vimentin-immunoreactive glial processes crossing a transverse line through the center of the fibrous scar tissue were counted. The mean and standard deviation (SD) were calculated from three fish, and significant differences were tested using the Mann–Whitney *U*-test.

Quantitative analysis of the morphological relationship between the axonal processes and glial processes within the fibrous scar

To determine whether glial elements play a guiding role for regenerating axons entering the scar, we examined the morphological relationship between acetylated tubulin-immunoreactive axonal processes and GFAP- and vimentin-immunoreactive glial processes, using a series of spinal cord sections obtained from the fish 3 days ($n=3$) after SCT. A total of

685 acetylated tubulin-immunoreactive axonal processes entering the fibrous scar were examined in 3 fish and the percentage of axons associated with GFAP- and vimentin-immunoreactive glial processes was calculated. The mean and SD were calculated from 3 fish.

Ethical statement

This study was carried out in accordance with the recommendations of The Yokohama City University Committee for Animal Research. All procedures were performed according to the standards established by the NIH Guide for the Care and Use of Laboratory Animals and the Policies on the Use of Animals and Humans in Research. All efforts were made to minimize the number of animals used and their suffering.

Results

Immunoreactivity of glial markers in intact spinal cord

In the intact spinal cord, BLBP-immunoreactive cellular structures were observed in the ependymo-radial glial cells lining the ependymal layer and in the subpial region, but not in other regions. BLBP-immunoreactive glial processes were observed in the parenchyma and subpial regions, primarily as radial processes extending from the ependymal layer (Fig. 1). Vimentin-immunoreactivity was observed at the luminal surface of the central canal, but not in the ependymo-radial glial cell bodies (Fig. 1). Vimentin-immunoreactive cellular structures were not observed in any other regions of the spinal cord, whereas vimentin-immunoreactive glial processes were observed in the parenchyma and subpial region, primarily as radial processes extending from the ependymal layer (Fig. 1). No GFAP-immunoreactivity was observed in cellular structures, including the ependymo-radial glial cells. Some GFAP-immunoreactive glial processes were observed in the parenchyma and subpial region, but not in the radial processes extending from the ependymal layer.

Immunoreactivity of glial markers in the lesioned spinal cord

After SCT, the open wound created by hemisection at the injury site was closed by a fibrous scar. The fibrous scar and surrounding nervous tissue were distinguished as areas with poor and strong GFAP-immunoreactivity, respectively (Figs. 2A, G and 3A).

Within 7 days after SCT, the fibrous scar was penetrated by a bundle of glial processes entering the scar from the surrounding nervous tissue (Fig. 2A–C). Within the bundle, GFAP-, vimentin-, and BLBP-immunoreactive glial processes were observed. Vimentin-immunoreactive glial processes, which were more numerous than GFAP-immunoreactive processes, were observed entering the fibrous scar even outside the bundle (Fig. 2B). Multiple labeling revealed that a majority of vimentin-immunoreactive and GFAP-immunoreactive glial processes were distinct, but some glial processes were immunoreactive for both GFAP and vimentin (Fig. 2D). Immunoreactivity for GFAP was observed in 15% of vimentin-immunoreactive glial processes and immunoreactivity for vimentin was observed in 26% of GFAP-immunoreactive glial processes (Fig. 2J). BLBP-immunoreactive glial processes were markedly fewer in number than vimentin- or GFAP-immunoreactive glial processes, and some were also immunoreactive for vimentin or GFAP (Fig. 2E, F). Within the bundle of glial processes entering the fibrous scar, many BLBP-immunoreactive cell bodies were also observed. Some of BLBP-immunoreactive cell bodies were positive for DAPI. No vimentin- or GFAP-immunoreactive cell bodies, on the other hand, were observed (Fig. 2G–I).

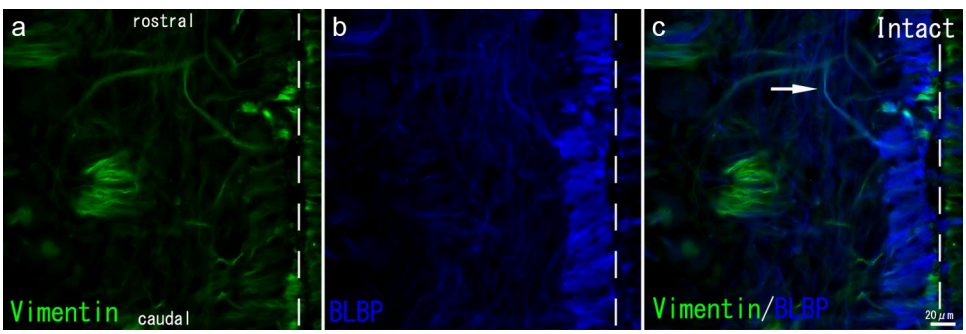

Fig. 1 Distribution of glial markers in the intact spinal cord. (**a**) Vimentin-immunoreactivity was observed on the luminal surface of the ependymo-radial glial cells. Vimentin-immunoreactivity was also observed in the radial processes (arrowheads) extending from the ependymal layer. (**b**) BLBP-immunoreactivity was observed in the ependymo-radial glial cell bodies (arrowheads) lining the ependymal layer and in the radial processes extending from the ependymal layer. (**c**) Merged image of (**a**) and (**b**). Radial processes immunoreactive for both vimentin and BLBP are indicated by an arrow. Dashed line: midline. Scale bars: 20 μm

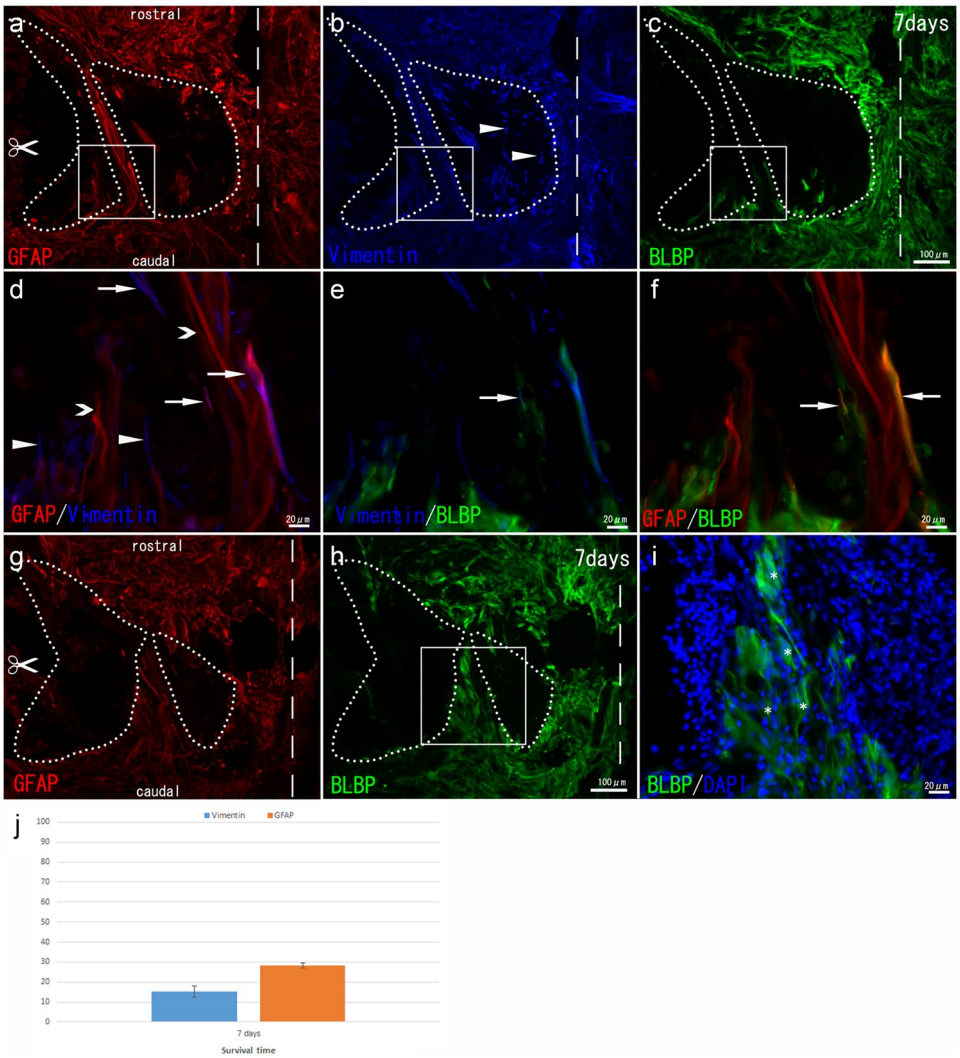

Fig. 2 Expression of glial markers at the injury site 7 days after SCT. A fibrous scar formed at the lesion center within 7 days after SCT. (**a**–**c**) Triple labeling of GFAP (red in (**a**)), vimentin (blue in (**b**)), and BLBP (green in (**c**)). A bundle of GFAP-, vimentin-, and BLBP-immunoreactive glial processes entered the fibrous scar from the surrounding nervous tissue and penetrated the scar. The area circled by the dotted line indicates the remaining fibrous scar. Many vimentin-immunoreactive glial processes (arrowheads in (**b**)) were observed entering the fibrous scar outside the bundle. (**d**–**f**) Enlarged images of the boxed regions in (**a**–**c**) are shown. Glial processes doubly immunoreactive for GFAP and vimentin (arrows in (**d**)), vimentin and BLBP (arrow in (**e**)), and GFAP and BLBP (arrows in (**f**)) were observed. Glial processes immunoreactive for GFAP, but not vimentin (chevron arrow in (**d**)), and those immunoreactive for vimentin, but not GFAP (arrowheads in (**d**)) were also observed. (**g**, **h**) Double labeling of GFAP (red in (**g**)), and BLBP (green in (**b**)). A bundle of GFAP- and BLBP-immunoreactive glial processes entered the fibrous scar from the surrounding nervous tissue and penetrated the scar. The area circled by the dotted line indicates the remaining fibrous scar. (**i**) An enlarged image of the boxed region in (**h**) is shown. BLBP-immunoreactive cell bodies (asterisks) were also positive for DAPI. Scissor marks in (**a**) and (**g**): hemisection site. Dashed line: midline. Scale bars: 100 μm in (**c**) and (**h**) (applies also to (**a**), (**b**), and (**g**)), 20 μm in (**f**) and (**i**) (applies also to (**d**) and (**e**)). (**j**) The ratio of glial processes doubly immunoreactive for GFAP and vimentin to total vimentin-immunoreactive glial processes and the ratio of glial processes doubly immunoreactive for GFAP and vimentin to total GFAP-immunoreactive glial processes at 7 days after SCT

Within 7 days after SCT, BLBP-immunoreactive cell bodies were also observed in the surrounding nervous tissue, as well as in the ependymo-radial glial cells lining the ependymal layer. No vimentin- or GFAP-immunoreactive cell bodies, including ependymo-radial glial cell bodies, were observed, even after SCT. Vimentin-immunoreactive glial processes were observed in the surrounding nervous tissue as well as in the radial processes originating from the ependymal layer. GFAP-immunoreactive glial processes were also observed in the surrounding nervous tissue, but not in the radial processes originating from the ependymal layer.

Morphological relationship between glial and axonal processes in the injury site

At the injury site, many glial processes entering the fibrous scar from the surrounding nervous tissue were accompanied by acetylated tubulin-immunoreactive axonal processes (Fig. 3A–F). Quantitative analysis revealed that the number of vimentin-immunoreactive processes at the injury center 3 and 7 days after SCT was significantly higher than the numbers of GFAP-immunoreactive glial processes and tubulin-immunoreactive axonal processes (Fig. 3G). Multiple labeling also revealed that a majority of vimentin-immunoreactive and GFAP-immunoreactive glial processes were distinct.

At 3 days after SCT, multiple labeling showed that many acetylated tubulin-immunoreactive axonal processes entering the fibrous scar were morphologically associated with glial processes. Some acetylated tubulin-immunoreactive axonal processes associated with GFAP-immunoreactive glial processes in the fibrous scar (Fig. 4A–C). Many acetylated tubulin-immunoreactive axonal processes associated with vimentin-immunoreactive glial processes (Fig. 4D–J). Acetylated tubulin-immunoreactive axonal processes

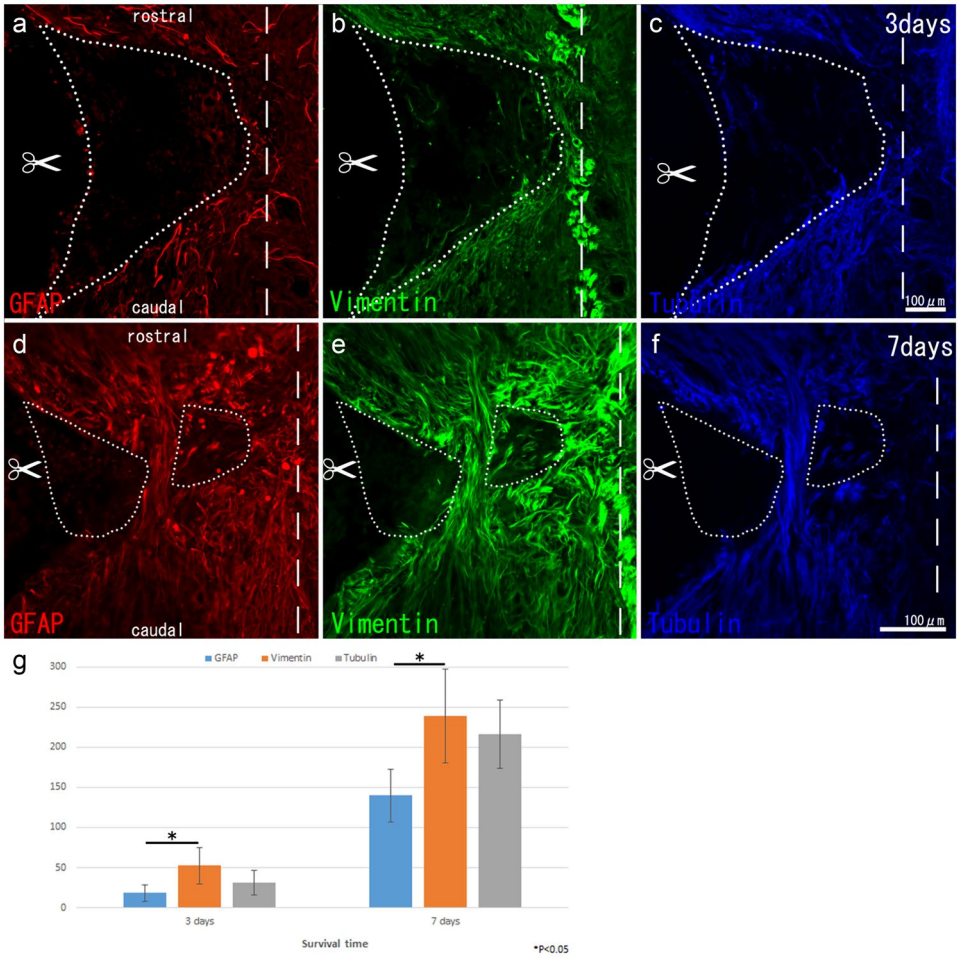

Fig. 3 Expression of glial and axonal markers at the injury site 3 and 7 days after SCT. (**a**–**c**) Triple labeling of GFAP (red in (**a**)), vimentin (green in (**b**)), and acetylated tubulin (blue in (**c**)) at the injury site 3 days after SCT. Vimentin-immunoreactive glial processes and acetylated tubulin-immunoreactive axons entered the fibrous scar at the lesion center. Vimentin-immunoreactive radial processes (shown in (**b**)) were observed in the midline. (**d**–**f**) Triple labeling of GFAP (red in (**d**)), vimentin (green in (**e**)), and acetylated tubulin (blue in (**f**)) at the injury site 7 days after SCT. The fibrous scar was penetrated by many glial processes immunoreactive for GFAP or vimentin and axonal processes immunoreactive for acetylated tubulin, and significantly reduced in area. The area circled by the dotted line indicates the remaining fibrous scar. Dashed line: midline. Scissor mark: hemisection site. Scale bars: 100 μm. (**g**) The numbers of acetylated tubulin-immunoreactive axonal processes, GFAP-immunoreactive glial processes, and vimentin-immunoreactive glial processes crossing a transverse line through the center of the fibrous scar 3 and 7 days after SCT. The number of vimentin-immunoreactive glial processes that reached the lesion center was significantly higher than the number of GFAP-immunoreactive glial processes. Values are means ± SD. Significant differences are indicated by * ($P < 0.05$)

associated with both vimentin-immunoreactive glial processes and GFAP-immunoreactive glial processes were frequently observed (Fig. 4J). Quantitative analysis showed that 1.7 ± 0.3% of acetylated tubulin-immunoreactive axonal processes associated with GFAP-immunoreactive glial processes, and 57.3 ± 4.4% of all acetylated tubulin-immunoreactive axonal processes associated with vimentin-immunoreactive glial processes. On the other hand, 18.3 ± 0.9% of acetylated tubulin-immunoreactive axonal processes associated with both vimentin- and GFAP-immunoreactive glial processes, and 22.3 ± 4.1% of acetylated tubulin-immunoreactive axonal processes associated with neither vimentin- nor GFAP-immunoreactive glial processes (Fig. 4K).

Expression of MMPs in glial processes within the tubular structures

In the fibrous scar at 7 days after SCT, MMP-14 was frequently detected in vimentin-immunoreactive glial processes. MMP-9, however, was not expressed in vimentin-immunoreactive glial processes (Fig. 5). MMP-14 was occasionally expressed in GFAP-immunoreactive processes. MMP-9 was observed in the fibrous scar, but not expressed in GFAP-immunoreactive processes.

Discussion

Spontaneous recovery after SCT in goldfish is unique in that regenerating axons pass through the fibrous scar that forms at the injury site (Bernstein 1964; Bernstein and Bernstein 1967; Takeda et al. 2015). This regeneration process contrasts with that in zebrafish, urodeles, and a freshwater turtle, in which no scar forms and regenerating axons grow on glial bridges created by elongated glial cells (Chernoff et al. 2003; Goldshmit et al. 2012; Rehermann et al. 2009; Zukor et al. 2011). Previous studies in goldfish demonstrated that the tubular structures protruding from the surrounding nervous tissue into the fibrous scar provide a passageway for regenerating axons and glial processes, but it is unclear whether glial elements guide the outgrowth of regenerating axons through the tubular structures (Takeda et al. 2015).

The present study revealed that many vimentin-positive glial processes entered the fibrous scar along with acetylated tubulin-positive axonal processes within 3 days after SCT. Although GFAP-positive processes also entered the tubular structures, they were fewer in number. Many of the vimentin-positive glial processes were not positive for GFAP, suggesting that they were largely distinct, although some were doubly positive. Vimentin-positive glial processes frequently associated with acetylated tubulin-positive axonal processes in the fibrous scar. The percentage of acetylated tubulin-positive axonal processes associated with vimentin-positive glial processes was significantly higher than the percentage of axonal processes associated with GFAP-positive glial processes. Regenerating axons entering the fibrous scar through the tubular structures, therefore, are much more frequently associated with vimentin- than with GFAP-positive glial processes. The present results also suggest that some regenerating axons are associated with glial processes doubly positive for vimentin and GFAP, but more regenerating axons are associated with both vimentin- and GFAP-positive glial processes.

Based on the GFAP-immunoreactivity, regenerating axons in goldfish after SCT were previously considered to grow through the injury site without guidance from glial elements because GFAP-positive glial processes often grow behind axons (Nona and Stafford 1995). This view was supported not only in goldfish but also in eel and zebrafish, where glial bridges are created instead of scar tissue at the injury site (Dervan and Roberts 2003; Tsata and Wehner 2021). Fine glial processes extending from stem processes, however, are devoid of intermediate filaments such as GFAP and vimentin and contain only actin as a cytoskeletal element. Visualization of the tips of glial processes would require the examination of cell type–specific markers expressed in the cytoplasm of astrocyte processes, such as ezrin (Lavialle et al. 2011). Alternatively, glutamate synthase and aquaporin-4, which are expressed in zebrafish astrocytes (Grupp et al. 2010), may be useful markers. Further studies are needed to determine whether vimentin-positive glial elements have a role in guiding the outgrowth of regenerating axons.

The present results provide evidence for the origin of the vimentin-positive glial processes in the fibrous scar. In intact spinal cord, the cell bodies of ependymo-radial glial cells lining the ependymal layer express BLBP but not GFAP or vimentin, and the radial processes protruding from the ependymal layer express vimentin and BLBP, but not GFAP, suggesting that goldfish ependymo-radial glial cells normally express BLBP in their cell bodies, and vimentin or BLBP in their processes. BLBP-positive cell bodies were scattered in the fibrous scar and surrounding nervous tissue after SCT, suggesting that ependymo-radial glial cells migrate to the injury site and surround the nervous tissue following SCT. Thus, the vimentin-positive glial processes entering the fibrous scar might derive from BLBP-positive cell bodies that migrated into the fibrous scar or surrounding nervous tissue.

In zebrafish, GFAP is expressed in both the cell bodies and radial processes of ependymo-radial glial cells (Goldshmit et al. 2012). In contrast, in goldfish, GFAP-immunoreactivity was not observed in the cell bodies and radial processes of ependymo-radial glial cells, either in intact spinal cord or injury site. GFAP-positive processes observed in the intact spinal cord and in the fibrous scar and surrounding nervous tissue following SCT might derive from astroglia-like cells in the parenchyma but not ependymo-radial glial cells.

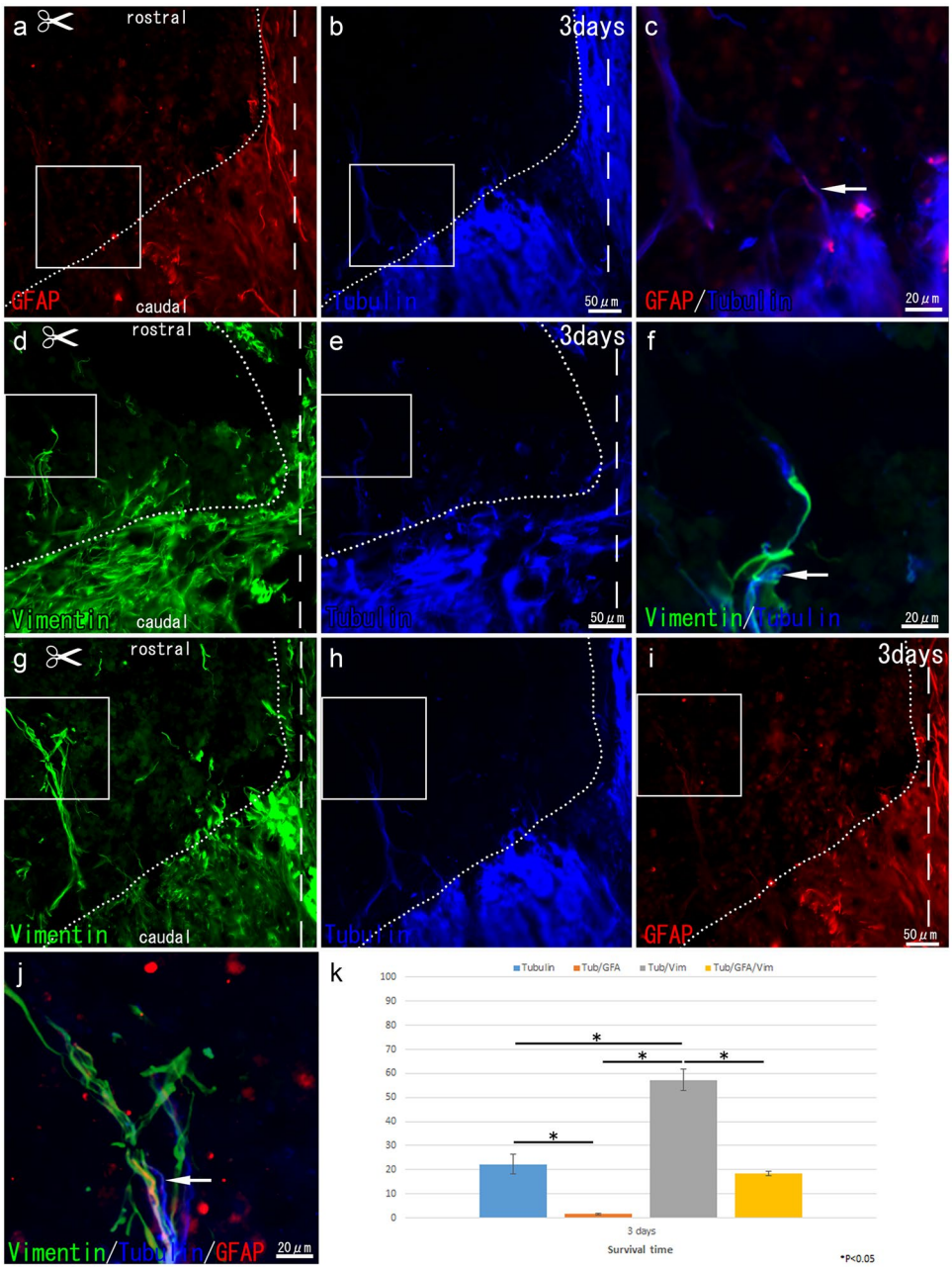

Fig. 4 The morphological relationship between acetylated tubulin-immunoreactive axonal processes and associated glial processes entering the fibrous scar 3 days after SCT. (**a**–**c**) Double labeling of GFAP (green in (**a**)), and acetylated tubulin (blue in (**b**)). A merged image of the enlarged area boxed in (**a**) and (**b**) is shown in (**c**). A GFAP-immunoreactive glial process was closely associated with an acetylated tubulin-immunoreactive axonal process (arrow). (**d**–**f**) Double labeling of vimentin (green in (**d**)), and acetylated tubulin (blue in (**e**)). A merged image of the enlarged area boxed in (**d**) and (**e**) is shown in (**f**). A vimentin-immunoreactive glial process was closely associated with an acetylated tubulin-immunoreactive axonal process (arrow). (**g**–**j**) Triple labeling of vimentin (green in (**g**)), acetylated tubulin (blue in (**h**)), and GFAP (red in (**i**)). A merged image of enlarged area boxed in (**g**–**i**) is shown in (**j**). Vimentin-immunoreactive glial processes and GFAP-immunoreactive glial processes were closely associated with an acetylated tubulin-immunoreactive axonal process (arrow). The area circled by the dotted line indicates the fibrous scar. Dashed line: midline. Scale bars: 50 μm in (**b**), (**e**), and (**i**) (apply also to (**a**), (**d**), (**g**), and (**h**)), and 20 μm in (**c**), (**f**), and (**j**). (**k**) Percentages of acetylated tubulin-immunoreactive axonal processes associated with vimentin-immunoreactive glial processes, those associated with GFAP-immunoreactive glial processes, those associated with both vimentin- and GFAP-immunoreactive glial processes, and those associated with neither vimentin- nor GFAP-immunoreactive glial processes, are shown. Values are means ± SD. Significant differences are indicated by * ($P < 0.05$)

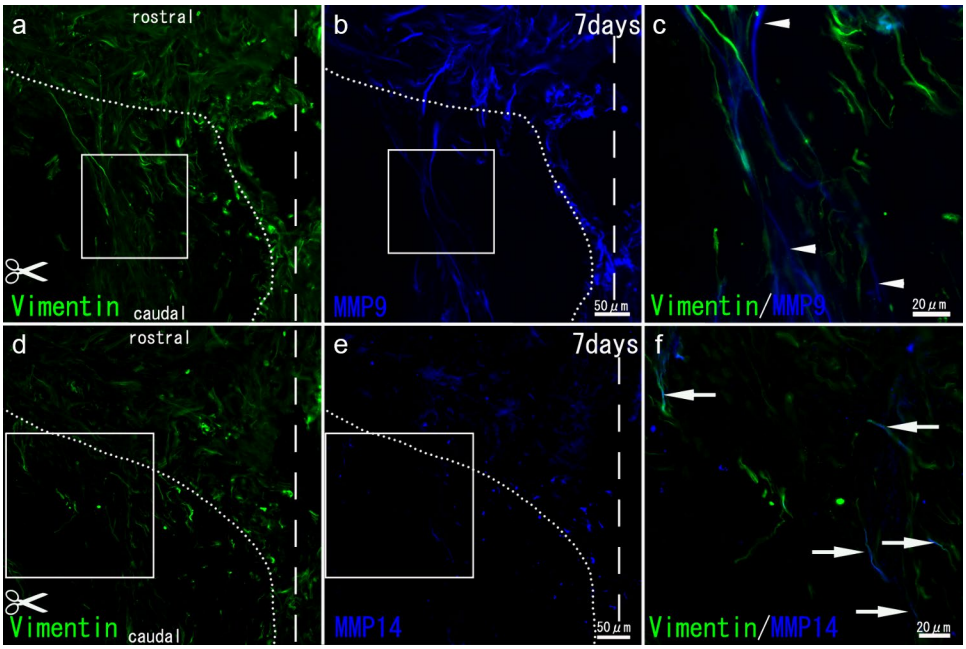

Fig. 5 Expression of MMPs in vimentin-immunoreactive glial processes in the fibrous scar. (**a**–**c**) Double labeling of vimentin (green in (**a**)), and MMP-9 (blue in (**b**)). A merged image of the enlarged area boxed in (**a**) and (**b**) is shown in (**c**). No vimentin-immunoreactive processes co-expressed MMP. Processes immunoreactive for MMP-9, but not vimentin are indicated by arrowheads. (**d**–**f**) Double labeling of vimentin (green in (**d**)) and MMP-14 (blue in (**e**)). A merged image of the enlarged area boxed in (**d**) and (**e**) is shown in (**f**). Vimentin-immunoreactive processes co-expressing MMP-14 are indicated by arrows. Dotted line: border between the nervous tissue and the fibrous scar. Dashed line: midline. Scale bars: 20 μm

Vimentin is an intermediate filament protein expressed primarily in mesenchymal cells but also in ependymo-radial glial cells and their radial processes in some adult teleosts, such as the gray mullet *Chelon labrosus* and the brown ghost knifefish *A. leptorhynchus* (Arochena et al. 2004; Zupanc et al. 2012). In the gray mullet, both vimentin and GFAP are expressed in the adult spinal ependymo-radial glial cells, but vimentin expression appears before GFAP expression during development (Arochena et al. 2004). In zebrafish, on the other hand, ependymo-radial glial cells express GFAP but not vimentin in intact spinal cord, but vimentin is transiently upregulated and GFAP is transiently downregulated at 3–5 days after SCT. The vimentin-positive ependymo-radial glial cells in zebrafish at this stage are bipolar and are involved in forming glial bridges. Regenerating axons pass through the injury site along the glial bridges when the ependymo-radial glial cells in the glial bridges re-express GFAP and vimentin expression is suppressed (Goldshmit et al. 2012). In zebrafish, therefore, vimentin-positive ependymo-radial glial cells might play an important role in inducing axonal regeneration, although their appearance is transient. The process of axonal regeneration after SCT in goldfish and zebrafish differs greatly depending on the presence or absence of scar tissue, but in both species, vimentin-positive ependymo-radial glial cells and their processes might contribute to axonal regeneration after SCT.

Axonal regeneration across the injury site also occurs after SCT in some urodele species, such as axolotl and newt, and in reptiles, such as freshwater turtle. In these animals, no scar tissue forms at the injury site, but rather the ependymo-radial glial cells create glial bridges or ependymal tubes that permit reconnection of the spinal cord (Chernoff et al. 2003; Rehermann et al. 2009; Zukor et al. 2011). In axolotl, the spinal cord gap is filled by the migrating de-differentiated ependymo-radial glial cells that re-epithelialize to form ependymal tubes and provide a scaffold for the long-axis growth of regenerating axons (Chernoff et al. 2003; O'Hara et al. 1992). In newt, the regenerating axons growing across the injury site are closely associated with GFAP-positive processes that might originate from the ependymo-radial glial cells or astrocytes (Zukor et al. 2011). In freshwater turtle, regenerating axons crossing the injury site travel on a scaffold comprising GFAP- and BLBP-positive radial glial cells and their processes running parallel to the regenerating axons (Rehermann et al. 2009). Together, these findings suggest that ependymo-radial glial cells are involved in axonal regeneration, but their precise roles in axonal regeneration are unclear. In axolotl, the ependymo-radial glial cells transiently express vimentin as they de-differentiate and migrate to the gap region (Chernoff et al. 2003). Further studies are needed to examine whether and how vimentin-positive ependymo-radial glial cells and their processes promote axonal regeneration in urodele and reptiles.

In the present study, MMP-14 was expressed in many vimentin-positive glial processes in the fibrous scar. We also observed MMP-14 expression in some GFAP-positive glial processes in the fibrous scar, consistent with findings reported by Takeda et al. (2021), who demonstrated MMP-14 expression in 6.3% of GFAP-positive glial processes at 2 weeks after SCT. MMP-9 and MMP-14 are also expressed in regenerating axons in the fibrous scar, suggesting that they degrade various extracellular matrix proteins such as collagens and chondroitin sulfate proteoglycans (Takeda et al. 2021). MMP-14 is an enzyme that resides in the plasma membrane and degrades substances contacting the plasma membrane (Hirsch et al. 1995). MMP-14 in vimentin-positive glial processes, along with MMPs in regenerating axons, might play a major role in the protrusion of nervous elements deeper into the fibrous scar by degrading extracellular matrix proteins to create a beneficial environment for axonal regeneration.

Acknowledgements We are grateful to Mrs. M. Kobayashi and Mr. Takuma Shibata for their expert technical aids.

Author contribution A.T. and M.T. acquired, analyzed, and interpreted the data and prepared the figures, and K.F. wrote the text of the manuscript. All authors reviewed the manuscript.

Funding This work is supported by the fundamental research funding of Yokohama City University.

Data availability No datasets were generated or analysed during the current study.

Declarations

Ethical approval This study was approved by The Yokohama City University Committee for Animal Research (approval NO. F-A-23–040).

Consent to participate Not applicable for this study.

Conflict of interest The authors declare no competing interests.

References

Adolf B, Chapouton P, Lam CS, Topp S, Tannhäuser B, Strähle U, Götz M, Bally-Cuif L (2006) Conserved and acquired features of adult neurogenesis in the zebrafish telencephalon. Dev Biol 295:278–293

Arochena M, Anadón R, Díaz-Regueira SM (2004) Development of vimentin and glial fibrillary acidic protein immunoreactivities in the brain of gray mullet (*Chelon labrosus*), an advanced teleost. J Comp Neurol 469:413–436

Becker T, Becker CG (2020) Dynamic cell interactions allow spinal cord regeneration in zebrafish. Curr Opin Physiol 14:64–69

Becker T, Wullimann MF, Becker CG, Bernhardt RR, Schachner M (1997) Axonal regrowth after spinal cord transection in adult zebrafish. J Comp Neurol 377:577–595

Becker CG, Lieberoth BC, Morellini F, Feldner J, Becker T, Schachner M (2004) L1.1 is involved in spinal cord regeneration in adult zebrafish. J Neurosci 24:7837–7842

Bernstein JJ (1964) Relation of spinal cord regeneration to age in adult goldfish. Exp Neurol 9:161–174

Bernstein JJ, Bernstein ME (1967) Effect of glial-ependymal scar and Teflon arrest on the regenerative capacity of goldfish spinal cord. Exp Neurol 19:25–32

Chernoff EAG, Stocum DL, Nye HLD, Cameron JA (2003) Urodele spinal cord regeneration and related processes. Dev Dyn 226:295–307

Dervan AG, Roberts BL (2003) Reaction of spinal cord central canal cells to cord transection and their contribution to cord regeneration. J Comp Neurol 458:293–306

Goldshmit Y, Sztal TE, Jusuf PR, Hall TE, Nguyen-Chi M, Currie PD (2012) Fgf-dependent glial cell bridges facilitate spinal cord regeneration in zebrafish. J Neurosci 32:7477–7492

Grupp L, Wolburg H, Mack AF (2010) Astroglial structures in the zebrafish brain. J Comp Neurol 518:4277–4287

Hirsch S, Cahill MA, Stuermer CAO (1995) Fibroblasts at the transection site of the injured goldfish optic nerve and their potential role during retinal axonal regeneration. J Comp Neurol 360:599–611

Koppanyi T (1955) Regeneration in the central nervous tissue of fish. In: Windle WF (ed) Regeneration in the central nervous system. Thomas Publisher, Springfield, Charles C, pp 3–19

Lavialle M, Aumann G, Anlauf E, Pröls F, Arpin M, Derouiche A (2011) Structural plasticity of perisynaptic astrocyte processes involves ezrin and metabotropic glutamate receptors. Proc Natl Acad Sci USA 108:12915–12919

Nona SN, Stafford CA (1995) Glial repair at the lesion site in regenerating goldfish spinal cord: an immunohistochemical study using species-specific antibodies. J Neurosci Res 42:350–356

O'Hara CM, Egar MW, Chernoff EA (1992) Reorganization of the ependyma during axolotl spinal cord regeneration: changes in intermediate filament and fibronectin expression. Dev Dyn 193:103–115

Rehermann MI, Marichal N, Russo RE, Trujillo-Cenóz O (2009) Neural reconnection in the transected spinal cord of the freshwater turtle *Trachemys dorbignyi*. J Comp Neurol 515:197–214

Sharma SC, Jadhao AG, Prasada Rao PD (1993) Regeneration of supraspinal projection neurons in the adult goldfish. Brain Res 620:221–228

Sun W, Cornwell A, Li J, Peng S, Osorio MJ, Aalling N, Wang S, Benraiss A, Lou N, Goldman SA, Nedergaard M (2017) SOX9 is an astrocyte-specific nuclear marker in the adult brain outside the neurogenic regions. J Neurosci 37:4493–4507

Takeda A, Goris RC, Funakoshi K (2007) Regeneration of descending projections to the spinal motor neurons after spinal hemisection in the goldfish. Brain Res 1155:17–23

Takeda A, Atobe Y, Kadota T, Goris RC, Funakoshi K (2015) Axonal regeneration through the fibrous scar in lesioned goldfish spinal cord. Neuroscience 284:134–152

Takeda A, Kanemura A, Funakoshi K (2021) Expression of matrix metalloproteinases during axonal regeneration in the goldfish spinal cord. J Chem Neuroanat 118:102041

Takeda A, Fujita M, Funakoshi K (2023) Distribution of 5HT receptors during the regeneration process after spinal cord transection in goldfish. J Chem Neuroanat 131:102281

Tsata V, Wehner D (2021) Know how to regrow-axon regeneration in the zebrafish. Cells 10:1404

Tsata V, Möllmert S, Schweitzer C, Kolb J, Möckel C, Böhm B, Rosso G, Lange C, Lesche M, Hammer J, Kesavan G, Beis D, Guck J, Brand M, Wehner D (2021) A switch in pdgfrb cell-derived ECM composition prevents inhibitory scarring and promotes axon regeneration in the zebrafish spinal cord. Dev Cell 56:509–524

Vitalo AG, Sîrbulescu RF, Ilieş I, Zupanc GK (2016) Absence of gliosis in a teleost model of spinal cord regeneration. J Comp Physiol A 202:445–456

Wen CM, Wang CS, Chin TC, Cheng ST, Nan FH (2010) Immunochemical and molecular characterization of a novel cell line derived from the brain of Trachinotus blochii (Teleostei, Perciformes): a fish cell line with oligodendrocyte progenitor cell and tanycyte characteristics. Comp Biochem Physiol A Mol Integr Physiol 156:224–231

Wilson SW, Ross LS, Parret T, Easter SS Jr (1990) The development of a simple scaffold of axon tracts in the brain of the embryonic zebrafish, *Brachydanio rerio*. Development 108:121–145

Zukor KA, Kent DT, Odelberg J (2011) Meningeal cells and glia establish a permissive environment for axon regeneration after spinal cord injury in newt. Neural Dev 6:1

Zupanc GKH (2019) Stem-cell-driven growth and regrowth of the adult spinal cord in teleost fish. Dev Neurobiol 79:406–423

Zupanc GKH, Sîrbulescu RF, Ilieş I (2012) Radial glia in the cerebellum of adult teleost fish: implications for the guidance of migrating new neurons. Neuroscience 210:416–430